Quantifying Functional Links between Brain and Heartbeat Dynamics in the Multifractal Domain: a Preliminary Analysis

Vincenzo Catrambone, Herwig Wendt, Riccardo Barbieri, Patrice Abry, Gaetano Valenza

Quantifying Functional Links between Brain and Heartbeat Dynamics in the Multifractal Domain: a Preliminary Analysis

Vincenzo Catrambone[*1], Herwig Wendt[2], Riccardo Barbieri[3], Patrice Abry[4], and Gaetano Valenza[1]

Abstract— **Quantification of brain-heart interplay (BHI) has mainly been performed in the time and frequency domains. However, such functional interactions are likely to involve nonlinear dynamics associated with the two systems. To this extent, in this preliminary study we investigate the functional coupling between multifractal properties of Electroencephalography (EEG) and Heart Rate Variability (HRV) series using a channel- and time scale-wise maximal information coefficient analysis. Experimental results were gathered from 24 healthy volunteers undergoing a resting state and a cold-pressure test, and suggest that significant changes between the two experimental conditions might be associated with nonlinear quantifiers of the multifractal spectrum. Particularly, major brain-heart functional coupling was associated with the second-order cumulant of the multifractal spectrum. We conclude that a functional nonlinear relationship between brain- and heartbeat-related multifractal sprectra exist, with higher values associated with the resting state.**

Clinical relevance: **The presented methodology could provide biomarkers for supporting the diagnosis of neurological, psychiatric, and cardiovascular disorders.**

I. Introduction

The central nervous system and the cardiovascular system continuously interact and communicate through anatomical, biochemical, and functional links, and the resulting functional network has been referred to as the central-autonomic network (CAN) [1]–[3].

Focusing on Electroencephalography (EEG) and Heart Rate Variability (HRV) series, previous studies investigated CAN-related changes between different populations and experimental conditions, and model-based and model-free approaches have been proposed. While a model-based approach exploits a-priori knowledge or assumptions to try to describe the functional brain-heart information exchange, a model-free approach focuses on synchronized brain and heartbeat events. Exemplarily, we recently proposed a model-based approach based on synthetic data generation for a functional directional brain-heart interplay assessment, which was evaluated with data gathered from healthy subjects undergoing relevant sympathovagal changes induced by a cold-pressor test [4]. On the other hand, exemplary model-free approaches

include the so-called Heartbeat-Evoked Potential (HEP) [5], the application of information theory methods applied to brain and heartbeat dynamics [6], and joint symbolic analysis [7].

The cardiovascular system shows a nonlinear and non-stationary behaviour due to several interactions with the respiratory and nervous systems [8]. Consequently, heartbeat dynamics has been successfully modelled by exploiting the so-called multifractal (MF) framework analysis through the definition of a *multifractal spectrum $D(h)$* characterizing transient and local non-Gaussian structures that a single Hurst exponent, H, may not describe [9]–[12]. Similarly, EEG series show multiple local singular behaviours going beyond self-similarity and thus need a model comprising a collection of exponents $H = h(t)$ to fully characterize its dynamics [13], [14]. Exemplarily, MF properties were investigated in several EEG studies on, e.g., sleep [15], motor imagery [16], and epileptic seizures [17], learning [18], and functional brain connectivity [19].

From an estimation viewpoint, the wavelet transform modulus maxima method [20], and the MF detrended fluctuation analysis [21] were proposed to estimate $D(h)$. Recently, we used a wavelet leader multifractal formalisms [22] and its generalization using p-leaders [23], [24] with non-gaussian expansion to characterize brain and heartbeat dynamics separately during a Cold-Pressor Test (CPT) [25], [26]. CPT comprises a strong thermal elicitation with consequent sympathovagal changes and was associated with significantly lower MF features derived from both EEG [26] and heartbeat dynamics [25] than resting state. Furthermore, the crucial role of preprocessing on heartbeat dynamics based on inhomogeneous point-process models has been demonstrated [25], [27].

Despite the significance of the aforementioned evidences, the functional link between brain and heartbeat dynamics at a MF level has not been investigated yet. To this end, in this preliminary study we report on a methodological attempt aimed to combine brain- and heartbeat-derived multifractal features at different time scales using a channel-wise Maximal Information Coefficient (MIC) analysis. Experimental results were gathered from healthy volunteers undergoing resting state and CPT, and are shown in terms of p-values topographic maps.

II. Materials and Methods

A. Experimental Setup

A 128-channel EEG and one-lead ECG were collected from thirty healthy volunteers (gender balanced, average age

[1] Bioengineering and Robotics Research Center E.Piaggio & Department of Information Engineering, School of Engineering, University of Pisa, Italy;

[2] IRIT-ENSEEIHT, Université de Toulouse, CNRS, France;

[3] Department of Electronics, Informatics and Bioengineering, Politecnico di Milano, Italy;

[4] Univ Lyon, ENS de Lyon, Univ Claude Bernard, CNRS, Laboratoire de Physique, Lyon, France;

[*] Corresponding author. Email at: *vincenzo.catrambone@ing.unipi.it*

of 26.7) with a 500Hz sampling rate. Signals were gathered through a Geodesic EEG Systems 300 (Electrical Geodesics, Inc.). All subjects declared to be healthy and right-handed, and signed an informed consent. The experimental procedure was approved by the local ethical committee. Data with significant artifacts gathered from six participants were not considered for further analyses.

Subjects underwent a $3\,\mathrm{min}$ resting state session followed by a $3\,\mathrm{min}$ Cold-Pressor Test (CPT) session with their left hand in iced water, and were free to stop the session in case of pain. Further information can be found in [4].

B. EEG and ECG Preprocessing

EEG preprocessing was applied to a subset of 90 channels over the scalp and followed the so-called HAPPE procedure, whose details are extensively reported in [28]. For each EEG channel, the power spectral density (PSD) was then derived within five standard frequency bands: $\delta \in [1-4]$, $\theta \in [4-8]$, $\alpha \in [8-12]$, $\beta \in [12-30]$ and $\gamma \in [30-70]$ (all expressed in Hz). The PSD was estimated by exploiting the well-known Welch method with a Hamming window of $2\,\mathrm{sec}$ with a moving step of $0.25\,\mathrm{sec}$, thus obtaining a $4\,\mathrm{Hz}$ sampling rate for the time-frequency representation.

The ECG was processed to derive heartbeat dynamics. R-wave events were automatically identified through the well-known Pan-Tompkins algorithm, and eventual algorithmic and physiological artefacts were corrected using a previously developed method based on point-process statistics [29]. According to our previous evidence [27], instantaneous first-order statistics for heartbeat dynamics were retrieved from the instantaneous mean of an inverse-Gaussian probability density function predicting R-wave events in time, $\mu_{\mathrm{RR}}(t)$, in line with an inhomogeneous point-process framework [27].

C. Multifractal analysis

The *wavelet spectrum* of self-similar models is defined as:

$$S_{d_X}(j, q = 2) = \frac{1}{n_j} \sum_{k=1}^{n_j} |d_X(j, k)|^q \simeq K 2^{jqH} \quad (1)$$

with a power-law exponent controlled by the well-known Hurst parameter H. Here, n_j is the number of $d_X(j, k)$ available at scale 2^j, and $d_X(j, k) = \langle \psi_{j,k} | X \rangle$ is a pattern of oscillation reference narrow in the time and frequency domains with *mother wavelet* ψ [30].

The wavelet spectrum is bounded to the Fourier spectrum, and H depends on linear data properties across frequency bands [10]. On the other hand, multifractal models build upon self-similarity by replacing the static parameter H with a collection of local exponents $H = h(t)$, and the *multifractal spectrum* $D(h)$ is then defined as the temporal repartition of $h(t)$ [10], [22]. The estimation of $D(h)$ from real data requires to impose $q = 2$ in (1) with positive and negative interval of moments q, and the use of wavelet p-leaders $\ell_X^{(p)}$:

$$\ell_X^{(p)}(j, k) = \left(2^j \sum_{\lambda' \subset 3\lambda_{j,k}} 2^{-j'} |d_X(\lambda')|^p \right)^{1/p} \quad (2)$$
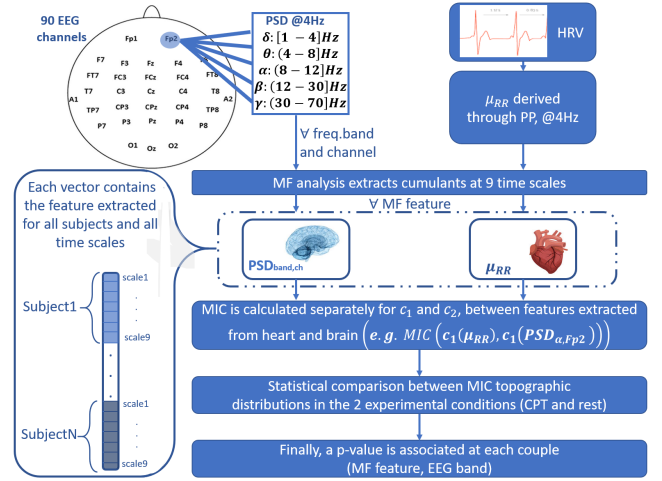

Fig. 1: Schematic representation of the implemented processing pipeline.

p-leaders $\ell_X^{(p)}$ are defined as ℓ^p norms of wavelet coefficients in a narrow temporal neighbourhood $\lambda_{j,k} = [k2^j, (k+1)2^j)$, with $3\lambda_{j,k} = \bigcup_{m\{-1,0,1\}} \lambda_{j,k+m}$, over all finer scales. Estimates from a multifractal spectrum $D(h)$ can be derived from the log-leaders cumulants as follows:

$$C_m^{(p)}(j) \equiv \mathrm{Cum}_m \log\left(\ell_X^{(p)}(j)\right) \simeq c_m^0 + c_m \log(2^j) \quad (3)$$

More specifically, the first-order cumulant c_1 identifies the H-related linear properties and the $D(h)$ mode, while the higher-order order cumulants c_2, c_3, c_4 represent nonlinear features from the multifractal spectrum such as width, asymmetry, and kurtosis. Further details are reported in [22]. In this preliminary study we limited our analysis to the first- and second-order cumulants c_1 and c_2.

D. Maximal Information Coefficient

MIC is an estimator of the linear and nonlinear coupling between pair of samples and is directly defined from the scatterplot of the two paired series, x and y [31]. A grid with any number of rows and columns can be superimposed to the scatterplot. Considering $G_{n_x \times n_y}$ as the set of all the possible partitions of that grid with n_x number of rows and n_y number of columns, the algorithm calculates the associated mutual information to all elements $g \in G_{n_x \times n_y}$ and finds the normalized maximum among G as follows:

$$m_{n_x \times n_y} = \frac{\max\limits_{g \in G_{n_x \times n_y}} \{I_g\}}{\log \min \{n_x, n_y\}} \quad (4)$$

MIC is then calculated as the maximal $m_{n_x \times n_y}$ over all the possible pairs (n_x, n_y). It has been found that MIC may also be estimated as: $MIC(x, y) = \max\limits_{n_x n_y < B} \{m_{n_x \times n_y}\}$, with B empirically defined as $B = n^{0.6}$. A fully detailed description is reported in [31].

E. Quantification of Functional Brain-Heart Interplay

For each of the twenty-four subjects and for each of the two experimental sessions, the two MF cumulants c_1 and c_2 were estimated separately from brain and heartbeat
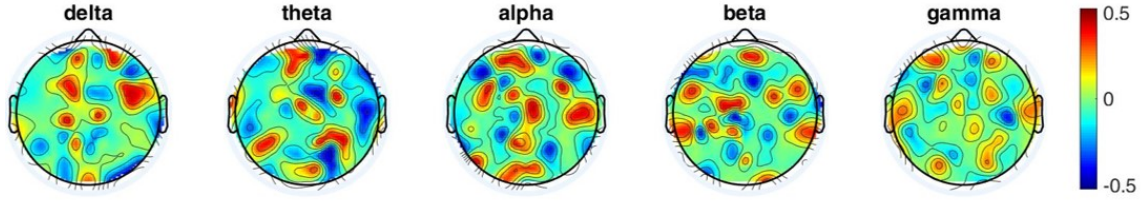
Fig. 2: Topographic distribution of MIC differences between CPT and resting phase for the first-order cumulant of the MF spectrum c_1 calculated between five EEG frequency powers and the first-order moment μ_{RR} derived from point-process models for heartbeat dynamics.
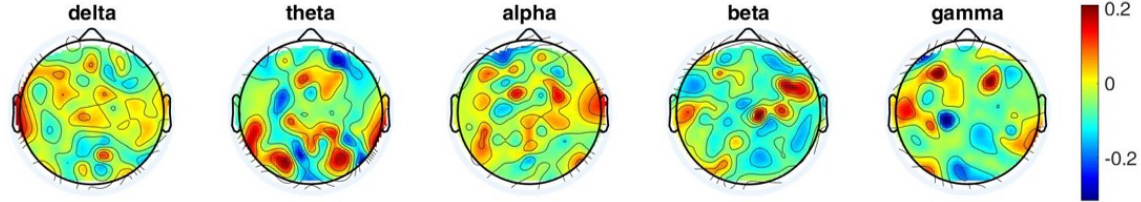

Fig. 3: Topographic distribution of MIC differences between CPT and resting phase for the second-order cumulant of the MF spectrum c_2 calculated between five EEG frequency powers and the first-order moment μ_{RR} derived from point-process models for heartbeat dynamics.

dynamics. Specifically, from the brain side, we calculated c_1 and c_2 for each of the 90 EEG channels and the 5 PSD time series at the standard frequency bands. From the heart side, we derived c_1 and c_2 associated with the μ_{RR} series. For each MF cumulants (c_1 and c_2) separately, a MIC was calculated group-wise between vectors whose length was of 216 elements, resulting from the number of subjects (i.e. 24) times the number of time scales (i.e. 9). Thus, a functional brain-heart interplay was quantified as $MIC_{c_1}(x,y)$ and $MIC_{c_2}(x,y)$, where x represents estimates from the heart side (e.g., $c_1(\mu_{RR})$) and y represents for estimates from the brain side at a specific frequency band and EEG channel (e.g., $c_1(PSD_{\alpha,Fp2})$). A schematic description of the analysis pipeline is reported in Figure 1.

Finally, separately for c_1 and c_2 and for each frequency band, statistically significant differences between the topographic distributions of MIC values (across the 90 EEG channels) extracted for the two experimental conditions (i.e. CPT and resting state) were investigated using Wilcoxon non-parametric tests for paired samples. The use of non-parametric tests was justified by the non-gaussian distribution of samples, as MIC may assume only positive values in the $[0-1]$ range.

The threshold for statistical significance was corrected in accordance with the Bonferroni rule considering a total of 10 multiple comparisons (5 EEG bands $\times$ 2 MF cumulants), thus $\alpha = \alpha^1/10 = 0.005$, with $\alpha = 0.05$ the uncorrected significance threshold.

III. EXPERIMENTAL RESULTS

Figures 2 and 3 show the topographic distribution of MIC differences between CPT and resting phase for c_1 and c_2, respectively. Particularly, while the c_1 parameter show non-specific patterns among channels with positive and negative values in the $[-0.5, 0.5]$ range, c_2 shows MIC values within

Fig. 4: Negative logarithm$_{10}$ of the $p-values$ from Wilcoxon non-parametric tests for the resting state vs. CPT comparison using MIC values at all EEG channels. Rows indicate MF cumulants, and columns indicate EEG-PSD frequency bands vs. μ_{RR}. Significant values are higher than $-log_{10}(\alpha = 0.005) = 2.301$.

a $[-0.2, 0.2]$ range with a prevalence for negative values (i.e., higher MIC values are associated with resting state), especially in the β and γ bands. Consequently, the functional relationship between brain and heart MF cumulants is higher during resting state than CPT.

Figure 4 shows the outcome of statistical comparisons between MIC values derived from resting state vs. CPT expressed in terms of $-log_{10}(P-value)$. The significance threshold is set to $-log_{10}(\alpha) = -log_{10}(0.005) = 2.301$ because of the Bonferroni correction. While no statistically significant comparisons are associated with the first-order MF cumulant c_1, several significant differences were found at all EEG frequency bands for c_2.

IV. DISCUSSION AND CONCLUSION

We reported on a novel methodology for quantifying brain-heart interplay based on functional relationships between MF cumulants. The method was tested on experimental EEG and heartbeat series gathered from 24 healthy volunteers undergoing a CPT elicitation that follows a resting state

session. Linear and nonlinear features were derived from the cumulants of the MF spectrum of brain and heartbeat series similarly to [25], [26], and their concurrent variation across time-scales was estimated through the MIC. Results suggest that significant statistical differences between the two experimental conditions may be associated with the nonlinear MF feature c_2, and no differences may be linked to the linear quantifier c_1. Higher c_2 values are in the resting state session with respect to the CPT session.

Previous studies investigated MF properties of EEG and heartbeat series separately during CPT and showed that the stressful condition leads to a decrease in MF properties towards a more linear dynamics [25], [26]. Here, we found that the functional coupling between brain- and heartbeat-derived MF metrics, quantified through MIC, follow the same trend as the single systems. These results confirm lower brain's and heart's multifractality during CPT than resting state, and suggest that a consistent decrease in their functional coupling exists in case of a CPT elicitation. On the other hand, linear properties of the MF spectrum (c_1) seem to be associated with a high inter-subject variability, therefore minimizing eventual statistical difference between experimental sessions. Note that p-values associated with the c_2 cumulant are as low as 10^{-8}, and more pronounced differences between the two experimental conditions are associated with higher EEG oscillations in the β and γ bands.

The proposed methodology presents a limitation related to the non-quantification of the directionality of the functional coupling between brain and heartbeat dynamics. Moreover, statistical analyses were performed at a channel-wise level, thus limiting any inference regarding specific brain regions.

This study represents a first attempt for the quantification of linear and nonlinear dependence between MF properties of brain and heartbeat dynamics. We conclude that a functional nonlinear relationship between brain- and heartbeat-related MF cumulants exist, and higher values are associated with the resting state than the CPT. Further endeavours will be directed to the investigation of other features derived from the MF spectrum, as well as to the application of physiological data collected during different experimental conditions.

REFERENCES

[1] G. Valenza *et al.*, "The central autonomic network at rest: Uncovering functional mri correlates of time-varying autonomic outflow," *NeuroImage*, vol. 197, pp. 383–390, 2019.

[2] F. Beissner, "The autonomic brain: an activation likelihood estimation meta-analysis for central processing of autonomic function," *Journal of Neuroscience*, vol. 33, no. 25, pp. 10503–10511, 2013.

[3] G. Valenza, L. Passamonti, A. Duggento, N. Toschi, and R. Barbieri, "Uncovering complex central autonomic networks at rest: a functional magnetic resonance imaging study on complex cardiovascular oscillations," *Journal of the Royal Society Interface*, vol. 17, no. 164, p. 20190878, 2020.

[4] V. Catrambone *et al.*, "Time-resolved directional brain-heart interplay measurement through synthetic data generation models," *Annals of Biomedical Engineering*, 2019.

[5] R. Schandry *et al.*, "From the heart to the brain: a study of heartbeat contingent scalp potentials," *International Journal of Neuroscience*, vol. 30, no. 4, pp. 261–275, 1986.

[6] L. Faes *et al.*, "Information dynamics of brain–heart physiological networks during sleep," *New Journal of Physics*, vol. 16, no. 10, p. 105005, 2014.

[7] S. Schulz *et al.*, "Central-and autonomic nervous system coupling in schizophrenia," *Philosophical Transactions of the Royal Society A: Mathematical, Physical and Engineering Sciences*, vol. 374, no. 2067, p. 20150178, 2016.

[8] K. Sunagawa *et al.*, "Dynamic nonlinear vago-sympathetic interaction in regulating heart rate," *Heart and vessels*, vol. 13, no. 4, pp. 157–174, 1998.

[9] P. Ivanov *et al.*, "Multifractality in human heartbeat dynamics," *Nature*, vol. 399, no. 6735, p. 461, 1999.

[10] M. Doret *et al.*, "Multifractal analysis of fetal heart rate variability in fetuses with and without severe acidosis during labor," *American journal of perinatology*, vol. 28, no. 04, pp. 259–266, 2011.

[11] T. Nakamur *et al.*, "Multiscale analysis of intensive longitudinal biomedical signals and its clinical applications," *Proc. IEEE*, vol. 104, no. 2, pp. 242–261, 2016.

[12] H. Wendt *et al.*, "Wavelet p-leader non gaussian multiscale expansions for heart rate variability analysis in congestive heart failure patients," *IEEE T. Biomedical Engineering*, vol. 66, no. 1, pp. 80–87, 2019.

[13] T. s Vicsek, *Fractal growth phenomena*. World scientific, 1992.

[14] H. Takayasu, *Fractals in the physical sciences*. Manchester University Press, 1990.

[15] I. Song *et al.*, "Multifractal analysis of sleep EEG dynamics in humans," in *Neural Engineering, 2007. CNE'07. 3rd IEEE/EMBS*, pp. 546–549, IEEE, 2007.

[16] D. Popivanov *et al.*, "Multifractality of decomposed EEG during imaginary and real visual-motor tracking," *Biological Cybernetics*, vol. 94, no. 2, pp. 149–156, 2006.

[17] Y. Zhang *et al.*, "Multifractal analysis and relevance vector machine-based automatic seizure detection in intracranial EEG," *International journal of neural systems*, vol. 25, no. 06, p. 1550020, 2015.

[18] D. La Rocca *et al.*, "Self-similarity and multifractality in human brain activity: a wavelet-based analysis of scale-free brain dynamics," *Journal of neuroscience methods*, vol. 309, pp. 175–187, 2018.

[19] P. Ciuciu, P. Abry, and B. He, "Interplay between functional connectivity and scale-free dynamics in intrinsic fmri networks," *Neuroimage*, vol. 95, pp. 248–263, 2014.

[20] J. Muzy *et al.*, "Multifractal formalism for fractal signals: The structure-function approach versus the wavelet-transform modulus-maxima method," *Physical review E*, vol. 47, no. 2, p. 875, 1993.

[21] J. Kantelhardt *et al.*, "Multifractal detrended fluctuation analysis of nonstationary time series," *Physica A: Statistical Mechanics and its Applications*, vol. 316, no. 1-4, pp. 87–114, 2002.

[22] H. Wendt *et al.*, "Bootstrap for empirical multifractal analysis," *IEEE signal processing magazine*, vol. 24, no. 4, pp. 38–48, 2007.

[23] S. Jaffard *et al.*, "p-exponent and p-leaders, part i: Negative pointwise regularity," *Physica A: Statistical Mechanics and its Applications*, vol. 448, pp. 300–318, 2016.

[24] R. Leonarduzzi *et al.*, "p-exponent and p-leaders, part ii: Multifractal analysis. relations to detrended fluctuation analysis.," *Physica A*, vol. 448, pp. 319–339, 2016.

[25] V. Catrambone *et al.*, "Heartbeat dynamics analysis under cold-pressure test using wavelet p-leader non-gaussian multiscale expansions," in *2019 41st Annual International Conference of the IEEE Engineering in Medicine and Biology Society (EMBC)*, pp. 2023–2026, IEEE, 2019.

[26] V. Catrambone *et al.*, "Wavelet p-leader non-gaussian multiscale expansions for eeg series: an exploratory study on cold-pressor test," in *2019 41st Annual International Conference of the IEEE Engineering in Medicine and Biology Society (EMBC)*, pp. 7096–7099, IEEE, 2019.

[27] G. Valenza *et al.*, "Mortality prediction in severe congestive heart failure patients with multifractal point-process modeling of heartbeat dynamics," *IEEE Transactions on Biomedical Engineering*, 2018.

[28] L. Gabard-Durnam *et al.*, "The harvard automated processing pipeline for electroencephalography (happe): standardized processing software for developmental and high-artifact data," *Frontiers in neuroscience*, vol. 12, p. 97, 2018.

[29] L. Citi *et al.*, "A real-time automated point-process method for the detection and correction of erroneous and ectopic heartbeats," *IEEE transactions on biomedical engineering*, vol. 59, no. 10, pp. 2828–2837, 2012.

[30] S. Mallat, *A wavelet tour of signal processing*. Elsevier, 1999.

[31] D. Reshef *et al.*, "Detecting novel associations in large data sets," *science*, vol. 334, no. 6062, pp. 1518–1524, 2011.